

Measurement of the τ anomalous magnetic moment by the CMS experiment

Izaak Neutelings* on behalf of the CMS collaboration

CERN,

Esplanade des Particules 1, Geneva, Switzerland

E-mail: izaak.neutelings@cern.ch

The photon-induced production of τ leptons has been measured by the CMS collaboration in both lead-lead and proton-proton collisions, at center-of-mass energies of $\sqrt{s_{NN}} = 5.02$ TeV and $\sqrt{s} = 13$ TeV, respectively. This was the first time such a process has been measured in proton-proton collisions. The results were also interpreted in terms of beyond-the-Standard-Model contributions to the anomalous electromagnetic moment of the τ lepton, setting the constraint $-0.0042 < a_\tau < 0.0062$ at 95% confidence level, improving the constraints set at LEP over 20 years ago.

*42nd International Conference on High Energy Physics (ICHEP2024)
18-24 July 2024
Prague, Czech Republic*

*Speaker

1. Introduction

The g -factor of the magnetic moment of leptons is predicted to be 2 by the Dirac equation, but is slightly larger due to quantum corrections. At next-leading order in quantum electrodynamics, the one-loop correction is given by the famous Schwinger term, $a = (g - 2)/2 = \alpha/2\pi$, and one can compute other contributions predicted by the Standard Model (SM) to high precision. Precision measurements of this basic particle property could reveal physics beyond the Standard Model (BSM). The electron magnetic moment was measured in Penning traps with a stunning precision of 0.13 parts per trillion, and agrees with the SM to about 1 in 13 decimal places [1], making it the most precise and accurate test of the SM. The magnetic moment of the muon is measured in storage rings due to its extremely short lifetime. Nevertheless, Fermilab has achieved very precise measurements up to about 0.22 parts per million [2]. There has been a longstanding tension between the measured values and some theoretical calculations up to 5 standard deviations (s.d.), which recent lattice QCD calculations may help partially resolve.

With a lifetime of about 2.9×10^{-13} s, the magnetic moment of the τ lepton cannot be measured from its oscillations in magnetic fields like for the electron and muon. The magnetic moment, as well as the electric dipole moment, of the τ lepton can however be probed indirectly from the $\gamma\tau\tau$ vertex. The most stringent constraints of $-0.052 < a_\tau < 0.013$ at 95% confidence level (CL), about 20 times the Swinger term, were set by the DELPHI Collaboration in 2004 in photon-induced production of a pair of τ leptons, $e^+e^- \rightarrow e^+e^-\tau\tau$ [3]. The $\gamma\gamma \rightarrow \tau^+\tau^-$ process has also been observed in lead-lead (PbPb) collisions at the LHC ($\text{PbPb} \rightarrow \text{Pb}^{(*)}\text{Pb}^{(*)}\tau\tau$, Fig. 1) in 2022, which has been used to place constraints on the τ anomalous magnetic moment, a_τ [4, 5]. Most recently, the CMS Collaboration [6] has observed $\gamma\gamma \rightarrow \tau^+\tau^-$ in proton-proton (pp) collisions for the first time ($\text{pp} \rightarrow \text{p}^{(*)}\text{p}^{(*)}\tau\tau$), and derived constraints on a_τ [7]¹. By using an EFT-approach, this analysis was also able to probe the electric dipole moment of the τ lepton, d_τ , which is extremely suppressed in the SM, but could be significantly enhanced by BSM contributions.

This proceeding will discuss the observations of the $\gamma\gamma \rightarrow \tau^+\tau^-$ and the subsequent measurement of the τ anomalous magnetic moment in PbPb and pp collisions at the CMS experiment, focussing on the new results in pp collisions.

2. $\gamma\gamma \rightarrow \tau\tau$ in PbPb collisions

With an atom number of $Z = 82$, the cross section of photon-fusion in PbPb collisions is enhanced by a factor Z^4 with respect to pp collisions. Analyses of photon-induced processes use ultra-peripheral collision (UPC) events of nuclei to obtain a very clean search channel. In UPC events, the lead nuclei collide with an impact parameter larger than the nucleus diameter, such that they are scattered or dissociated in the very forward direction. They are characterized by very low-track multiplicity and small backgrounds.

The CMS analysis uses the data set collected in 2015 at a center-of-mass energy per nucleon pair of $\sqrt{s_{\text{NN}}} = 5.02$ TeV corresponding to an integrated luminosity of $404 \mu\text{b}^{-1}$. It selects events with little to no activity in the forward detectors, and with the $\tau\tau$ final state where one τ lepton decays to a muon with two neutrinos, and the other to three charged hadrons with one neutrino. The $\gamma\gamma \rightarrow \tau^+\tau^-$ signal can clearly be observed in the distribution of the invariant mass of the visible $\tau\tau$ system in Fig. 1. The analysis estimates $-0.0079 < a_\tau < 0.0065$ at 68% CL, extracted from the total $\gamma\gamma \rightarrow \tau^+\tau^-$ cross section. More details can be found in Ref. [4].

¹This analysis has been published in Reports on Progress in Physics shortly after ICHEP2024 [7].

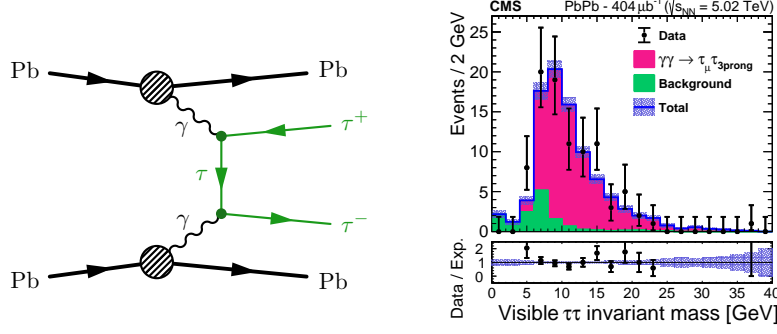


Figure 1: Feynman diagram of $\gamma\gamma \rightarrow \tau^+\tau^-$ in PbPb collisions (left). The invariant mass of the visible $\tau\tau$ system (right). The signal component (magenta) is stacked on top of the background component (green). The shaded area shows the statistical uncertainty. From Ref. [4].

3. $\gamma\gamma \rightarrow \tau\tau$ in pp collisions

The measurement of $\gamma\gamma \rightarrow \tau^+\tau^-$ in pp collisions does not enjoy the same Z^4 enhancement of the cross section seen in a PbPb analysis, and the events are not as clean because of large backgrounds, such as Drell–Yan (DY, $Z/\gamma^* \rightarrow \ell^+\ell^-$) and quark/gluon jets misidentified as hadronically decayed τ leptons. The higher rate of additional pp collisions per event (pileup, PU) in the pp data collected at $\sqrt{s} = 13$ TeV during Run 2 further increases hadronic activity around the signal. Furthermore, the signal efficiency is limited by the transverse momentum (p_T) thresholds of the CMS trigger. Nevertheless, the Run-2 pp data set used in the pp analysis [7] is about 137 fb^{-1} , about 8 orders of magnitude larger than the 2015 PbPb data set used by Ref. [4], and the pp analysis exploits more $\tau\tau$ final states. More importantly, while the PbPb analyses probe a phase space of $m_{\tau\tau} \lesssim 40 \text{ GeV}$ where the $\gamma\gamma \rightarrow \tau^+\tau^-$ cross section is larger, the phase space of the pp analysis ranges between $50 \text{ GeV} \lesssim m_{\tau\tau} \lesssim 500 \text{ GeV}$, where any BSM modifications of a_τ are enhanced. This fact allows the pp analysis to set more stringent constraints on a_τ .

3.1 Analysis strategy

Similar to UPC events, the colliding protons that generate photon-induced processes tend to scatter or dissociate in the forward direction, leaving little to no hadronic activity from the underlying event in the detector around the interaction vertex. The $\gamma\gamma \rightarrow \tau^+\tau^-$ signature is therefore τ leptons of opposite-sign charge that are back-to-back in the transverse plane (i.e., $|\Delta\phi| \approx \pi$) due to the lack of recoil, and with low track multiplicity around the $\tau\tau$ vertex.

The pp analysis targets in total four final states of a τ lepton pair (omitting the neutrinos): $e\mu$, $e\tau_h$, $\mu\tau_h$, and $\tau_h\tau_h$, where τ_h denotes the hadronic decay of a τ lepton. The $\mu\mu$ final state is used to derive various corrections to signal and background simulation, as explained in Section 3.3. To ensure the two τ decay candidates have a back-to-back topology, events are required to have $A = 1 - |\Delta\phi|/\pi < 0.015$ in the signal region (SR), where A is the so-called acoplanarity. Finally, the (SR) is categorized into events with either no or exactly one additional track in a $\Delta z = 0.1 \text{ cm}$ window along the beam axis (z) and around the $\tau\tau$ vertex.

The $\gamma\gamma \rightarrow \tau^+\tau^-$ signal is extracted by fitting the signal simulation to the observed distribution of the invariant mass of the visible $\tau\tau$ system, denoted as m_{vis} . Constraints on both a_τ and d_τ are extracted from the fit of both the signal shape and normalization, which is parametrized using an approach with SM effective-field theory (SMEFT) explained in Section 3.2.

3.2 Signal simulation

Signal samples of elastic $\gamma\gamma \rightarrow \tau^+\tau^-$ are generated with the GAMMA-UPC generator [8]. Nonelastic contributions where at least one of the protons fragments, are not available in GAMMA-UPC, but are estimated from a $\mu\mu$ control region, see Section 3.3.

Previous analyses used form factors to extract a_τ , while the pp analysis uses a SMEFT approach to extract both a_τ and d_τ , as suggested in Ref. [9]. Deviations from the SM that modify the electromagnetic moments at tree level can be parametrized in terms of two dimension-6 operators with complex Wilson coefficients $C_{\tau B}$ and $C_{\tau W}$ and BSM scale Λ . After electroweak symmetry breaking, deviations of a_τ and d_τ from the SM predictions can be expressed as:

$$\delta a_\tau = \frac{2m_\tau}{e} \frac{\sqrt{2}v}{\Lambda^2} \text{Re}[C_{\tau\gamma}] \quad \text{and} \quad \delta d_\tau = \frac{\sqrt{2}v}{\Lambda^2} \text{Im}[C_{\tau\gamma}], \quad (1)$$

where $C_{\tau\gamma} = \cos\theta_W C_{\tau B} - \sin\theta_W C_{\tau W}$, $v \approx 246$ GeV is the Higgs vacuum expectation value, and θ_W is the weak mixing angle. The form factor formalism and the SMEFT approach are equivalent assuming momentum transfer $q^2 = 0$.

3.3 Corrections

Several corrections to simulation are derived from $\mu\mu$ events to improve modeling of the data. To improve the estimation of the number of additional tracks from PU or hard-scattering (HS), an $\mu\mu$ event sample around the Z peak with $|m_{\mu\mu} - m_Z| < 15$ GeV is used. The corrections are defined as the ratio between the number of track distributions in 0.1 cm windows along the beam axis of observed and simulated DY data. PU tracks are counted in windows far away from the $\mu\mu$ vertex as illustrated in Fig. 2. HS tracks are counted inside the window around the $\mu\mu$ vertex.

The simulated signal sample only contains central exclusive events where both protons stay intact. However, single- and double-dissociative processes have larger cross sections and can have the same exclusive signature. This nonelastic contribution (as well as any higher-order corrections) are estimated from a purified $\gamma\gamma \rightarrow \mu^+\mu^-$ sample in $\mu\mu$ data with SR-like requirements $A < 0.015$ and $N_{\text{tracks}} = 0$ or 1. The background consists mostly of DY, and is estimated inclusively from the $3 \leq N_{\text{tracks}} \leq 5$ side band and normalized to the Z resonance separately in the $N_{\text{tracks}} = 0$ and 1 regions. The elastic $\gamma\gamma \rightarrow \mu^+\mu^-$, WW simulation is fitted to data after subtracting the inclusive backgrounds. As can be seen from the bottom panel in Fig. 3, a flat fit yields a rescaling factor of about 2.7. However, a $m_{\mu\mu}$ -dependence is found, and the linear fit is applied to all simulated photon-induced processes in the analysis, while the flat fit is used to derive a conservative shape uncertainty.

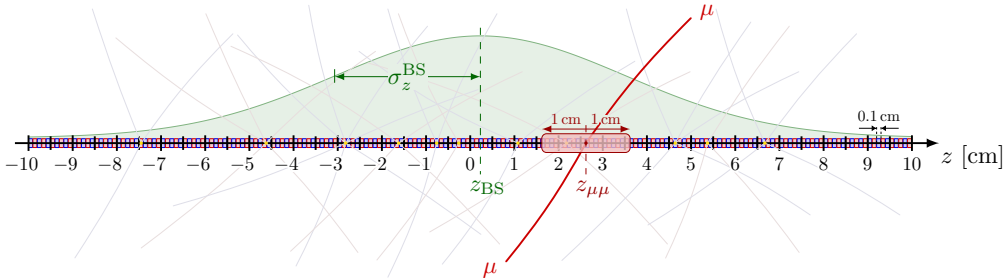


Figure 2: Schematic view of the 0.1 cm wide windows probed along the z axis to derive corrections to the pileup track density in simulation. The green distribution represents the gaussian beamspace profile.

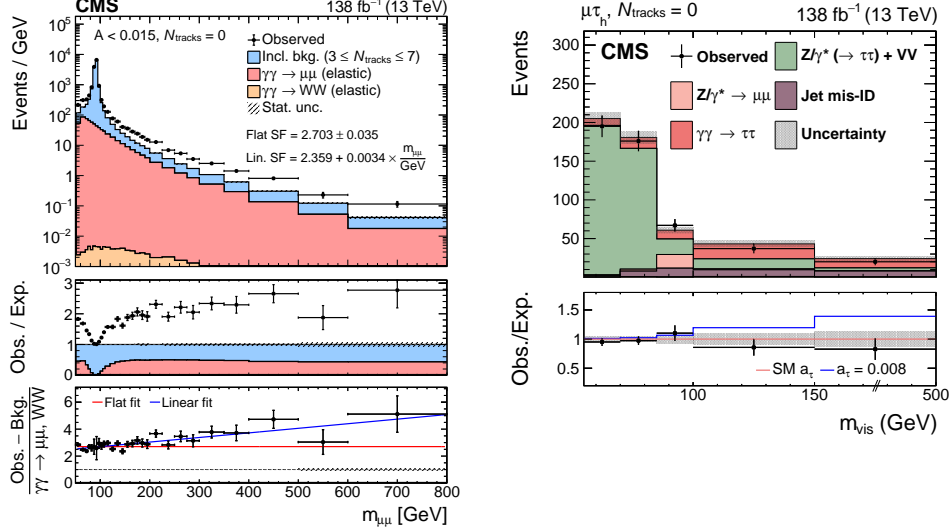


Figure 3: Measurement of the rescaling of the elastic exclusive signal in $\mu\mu$ events with $N_{\text{tracks}} = 0$, $A < 0.015$ (left). Bottom panel shows the flat (red) and linear fit (blue). Invariant mass of the visible $\tau\tau$ system in the SR of the $\mu\tau_h$ final state and $N_{\text{tracks}} = 0$ (right), with the $\gamma\gamma \rightarrow \tau^+\tau^-$ signal (pink). From Ref. [7].

3.4 Results

After performing a maximum likelihood fit to the observed m_{vis} distributions of each SR, and assuming the SM values of a_τ and d_τ , the $\gamma\gamma \rightarrow \tau^+\tau^-$ signal is observed with a significance of 5.3 s.d. The m_{vis} distribution in one of the eight SRs is shown in Fig. 3. The dominant systematic uncertainties are the elastic rescaling of the signal and the $N_{\text{tracks}}^{\text{HS}}$ correction to the DY background.

Constraints on a_τ and d_τ are set independently. The combined fit yields the constraints $-0.0022 < a_\tau < 0.0041$, at 68% CL ($-0.0042 < a_\tau < 0.0062$) at 68 (95)% CL, which is about five times more stringent than the next precise results by DELPHI, and about 2.7 times over the SM expectation. This corresponds to the measurement of the τ lepton magnetic moment at 0.3% precision, i.e. $g_\tau = 2.0018^{+0.0064}_{-0.0062}$. The constraints on d_τ are $|d_\tau| < 1.7 \times 10^{-17} \text{ ecm}$ ($|d_\tau| < 2.9 \times 10^{-17} \text{ ecm}$) at 68 (95)% CL, approaching the limits set by Belle. These results also allow to set constraints on the real and imaginary parts of the Wilson coefficients $C_{\tau B}$ and $C_{\tau W}$. A

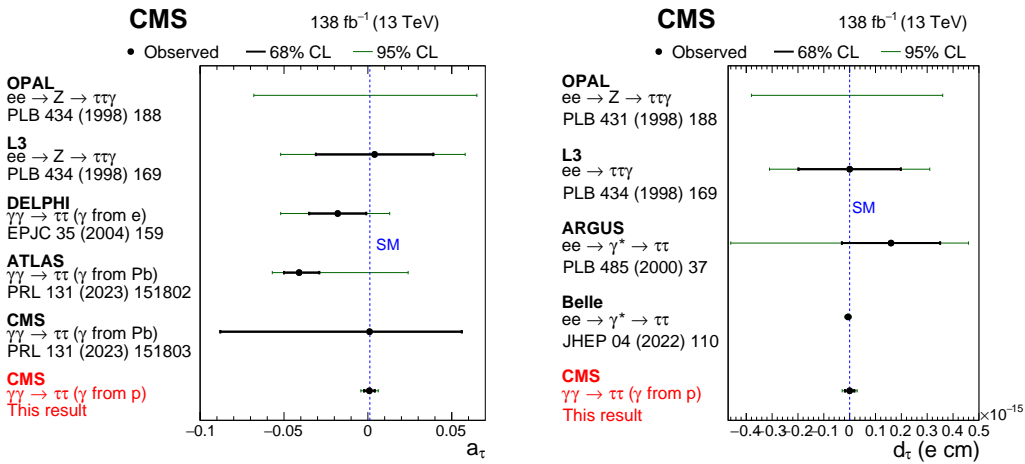


Figure 4: Measurements of a_τ (left) and d_τ (right) performed by Refs. [4] & [7], compared with previous results. From Ref. [7].

comparison of these results compared to previous ones are shown in Fig. 4.

4. Summary

Precision measurements of the anomalous magnetic moment of the τ lepton, a_τ , have a strong potential to probe new physics beyond the Standard Model. The ATLAS and CMS Collaborations have observed $\gamma\gamma \rightarrow \tau^+\tau^-$ in ultra-peripheral PbPb events, allowing them to set limits on a_τ . Recently, the CMS Collaboration has also observed for the first time $\gamma\gamma \rightarrow \tau^+\tau^-$ in proton-proton collisions with a significance of 5.3 standard deviations, by requiring a back-to-back topology of two τ leptons and no or exactly one track around the $\tau\tau$ vertex. Despite the smaller cross section than in PbPb, this analysis probes a phase space at $40 < m_{\tau\tau} < 500$ GeV, which is more sensitive to deviations from the SM of both a_τ and the electric dipole moment d_τ , allowing the pp analysis to set the strongest constraints on a_τ yet: $-0.0042 < a_\tau < 0.0062$ at 95% confidence level.

References

- [1] X. Fan, T. G. Myers, B. A. D. Sukra and G. Gabrielse, *Measurement of the Electron Magnetic Moment*, Phys. Rev. Lett. **130**, no.7, 071801 (2023), doi:[10.1103/PhysRevLett.130.071801](https://doi.org/10.1103/PhysRevLett.130.071801), [arXiv:2209.13084](https://arxiv.org/abs/2209.13084).
- [2] Muon g-2 Collaboration, *Measurement of the Positive Muon Anomalous Magnetic Moment to 0.20 ppm*, Phys. Rev. Lett. **131**, no.16, 161802 (2023), doi:[10.1103/PhysRevLett.131.161802](https://doi.org/10.1103/PhysRevLett.131.161802), [arXiv:2308.06230](https://arxiv.org/abs/2308.06230).
- [3] DELPHI Collaboration, *Study of tau-pair production in photon-photon collisions at LEP and limits on the anomalous electromagnetic moments of the tau lepton*, Eur. Phys. J. C **35**, 159-170 (2004), doi:[10.1140/epjc/s2004-01852-y](https://doi.org/10.1140/epjc/s2004-01852-y), [arXiv:hep-ex/0406010](https://arxiv.org/abs/hep-ex/0406010).
- [4] CMS Collaboration, *Observation of τ lepton pair production in ultraperipheral lead-lead collisions at $\sqrt{s_{NN}} = 5.02$ TeV*, Phys. Rev. Lett. **131**, 151803 (2023) doi:[10.1103/PhysRevLett.131.151803](https://doi.org/10.1103/PhysRevLett.131.151803), [arXiv:2206.05192](https://arxiv.org/abs/2206.05192).
- [5] ATLAS Collaboration, *Observation of the $\gamma\gamma \rightarrow \tau\tau$ Process in Pb+Pb Collisions and Constraints on the τ -Lepton Anomalous Magnetic Moment with the ATLAS Detector*, Phys. Rev. Lett. **131**, no.15, 151802 (2023) doi:[10.1103/PhysRevLett.131.151802](https://doi.org/10.1103/PhysRevLett.131.151802), [arXiv:2204.13478](https://arxiv.org/abs/2204.13478).
- [6] CMS Collaboration, *The CMS Experiment at the CERN LHC*, JINST **3** (2008), S08004 doi:[10.1088/1748-0221/3/08/S08004](https://doi.org/10.1088/1748-0221/3/08/S08004).
- [7] CMS Collaboration, *Observation of $\gamma\gamma \rightarrow \tau\tau$ in proton-proton collisions and limits on the anomalous electromagnetic moments of the τ lepton*, Rep. Prog. Phys. **87** 107801 (2024) doi:[10.1088/1361-6633/ad6fcb](https://doi.org/10.1088/1361-6633/ad6fcb), [arXiv:2406.03975](https://arxiv.org/abs/2406.03975).
- [8] H. S. Shao and D. d’Enterria, *gamma-UPC: automated generation of exclusive photon-photon processes in ultraperipheral proton and nuclear collisions with varying form factors*, JHEP **09**, 248 (2022), doi:[10.1007/JHEP09\(2022\)248](https://doi.org/10.1007/JHEP09(2022)248), [arXiv:2207.03012](https://arxiv.org/abs/2207.03012).
- [9] L. Beresford and J. Liu, *New physics and tau g – 2 using LHC heavy ion collisions*, Phys. Rev. D **102**, no.11, 113008 (2020) [erratum: Phys. Rev. D **106**, no.3, 039902 (2022)], doi:[10.1103/PhysRevD.102.113008](https://doi.org/10.1103/PhysRevD.102.113008), [arXiv:1908.05180](https://arxiv.org/abs/1908.05180).